Acta Pharmaceutica Sinica B 2024;14(6):2598–2612

Chinese Pharmaceutical Association
Institute of Materia Medica, Chinese Academy of Medical Sciences

Acta Pharmaceutica Sinica B

www.elsevier.com/locate/apsb
www.sciencedirect.com

ORIGINAL ARTICLE

Allosterically activating SHP2 by oleanolic acid inhibits STAT3–Th17 axis for ameliorating colitis

Jinbo Hu[a,†], Wen Liu[a,*,†], Yi Zou[b,†], Chenyang Jiao[a], Jiazhen Zhu[a], Qiang Xu[a], Jianjun Zou[b,*], Yang Sun[a,c,*], Wenjie Guo[a,*]

[a]*State Key Laboratory of Pharmaceutical Biotechnology, Nanjing Drum Tower Hospital, School of Life Sciences, Nanjing University, Nanjing 210093, China*
[b]*Department of Clinical Pharmacology, Nanjing First Hospital, Nanjing Medical University, Nanjing 210006, China*
[c]*Jiangsu Key Laboratory of New Drug Research and Clinical Pharmacy, Xuzhou Medical University, Xuzhou 221004, China*

Received 7 October 2023; received in revised form 21 December 2023; accepted 28 February 2024

KEY WORDS

Oleanolic acid;
SHP2;
STAT3;
Th17;
Colitis;
Allosteric activator

Abstract Src homology 2 domain-containing tyrosine phosphatase 2 (SHP2) is an essential tyrosine phosphatase that is pivotal in regulating various cellular signaling pathways such as cell growth, differentiation, and survival. The activation of SHP2 has been shown to have a therapeutic effect in colitis and Parkinson's disease. Thus, the identification of SHP2 activators and a complete understanding of their mechanism is required. We used a two-step screening assay to determine a novel allosteric activator of SHP2 that stabilizes it in an open conformation. Oleanolic acid was identified as a suitable candidate. By binding to R362, K364, and K366 in the active center of the PTP domain, oleanolic acid maintained the active open state of SHP2, which facilitated the binding between SHP2 and its substrate. This oleanolic acid-activated SHP2 hindered Th17 differentiation by disturbing the interaction between STAT3 and IL-6Rα and inhibiting the activation of STAT3. Furthermore, *via* the activation of SHP2 and subsequent attenuation of the STAT3–Th17 axis, oleanolic acid effectively mitigated colitis in mice. This protective effect was abrogated by SHP2 knockout or administration of the SHP2 inhibitor SHP099. These findings underscore the potential of oleanolic acid as a promising therapeutic agent for treating inflammatory bowel diseases.

*Corresponding authors.
E-mail addresses: zoujianjun100@126.com (Jianjun Zou), liuwen@nju.edu.cn (Wen Liu), yangsun@nju.edu.cn (Yang Sun), guowj@nju.edu.cn (Wenjie Guo).
[†]These authors made equal contributions to this work.
Peer review under the responsibility of Chinese Pharmaceutical Association and Institute of Materia Medica, Chinese Academy of Medical Sciences.

https://doi.org/10.1016/j.apsb.2024.03.017

1. Introduction

Crohn's disease is a chronic inflammatory condition that primarily affects the gastrointestinal tract. It is classified as one of the two main forms of inflammatory bowel disease, with the other being ulcerative colitis; both of which contribute substantially to severe pain, disability, and decreased overall quality of life. Crohn's disease can affect any part of the digestive system from the mouth to the anus but most commonly involves the end of the small intestine (ileum) and the beginning of the large intestine (colon)[1]. The hallmark of Crohn's disease is inflammation that extends throughout the thickness of the affected bowel wall, thus resulting in the formation of deep and painful ulcers. This inflammation may occur in a patchy manner with healthy tissues interspersed between the affected areas. Ongoing inflammation and ulceration can lead to various complications, such as narrowing of the intestine (strictures), formation of abnormal passages between organs (fistulas), and development of abscesses[2]. The exact cause of Crohn's disease is unknown; however, it is believed to be the result of an abnormal immune response to environmental triggers in individuals with a genetic predisposition. Factors, such as genetics, environmental factors (including diet and stress), and dysregulation of the gut microbiota, may play a role in its development[3].

Currently, there is no cure for Crohn's disease, and the condition typically follows a relapsing and remitting course. Treatment aims to control inflammation, alleviate symptoms, and improve patients' quality of life. Medical therapies often include anti-inflammatory drugs, immunosuppressants, biologics, and in some cases, corticosteroids during flare-ups[4,5]. In severe cases or when complications arise, surgery may be necessary to remove the affected parts of the intestine or to manage complications[6].

Src homology 2 domain-containing tyrosine phosphatase 2 (SHP2), a non-receptor tyrosine phosphatase, plays a crucial role in cell signaling and is closely linked to inflammation. The full-length SHP2-WT contains three domains: a protein tyrosine phosphatase (PTP) domain, two tandem SH2 domains (N-SH2 and C-SH2 domains), and a C-terminal tail. Undisturbed SHP2 exists in an auto-inhibited state, with the D'E loop of N-SH2 extending deep into the catalytic cleft of the PTP domain. Previous studies have demonstrated that SHP2 negatively regulates inflammation. For instance, SHP2 deletion in intestinal epithelial cells led to hyperactivation of inflammatory transcription factors STAT3 and NF-κB, thus resulting in elevated expression of epithelial chemokines and cytokines[7]. In T cells, SHP2 acts as a negative regulator of the IFN-γ-STAT1 and IL-6-STAT3 pathways, thereby reducing inflammation and preventing tumorigenesis[8]. SHP2 also promotes PD1-mediated T cell immunosuppression *via* interaction of the C-SH2 and N-SH2 domains with the ITSM and ITIM motifs of PD1, respectively[9]. In addition, our previous study demonstrated that SHP2 inhibited the activation of the NLRP3 inflammasome by maintaining mitochondrial homeostasis and preventing the release of mitochondrial DNA and reactive oxygen species[10]. These findings suggest that SHP2 is a promising anti-inflammatory target, and the identification of SHP2 activators can help develop a novel strategy for anti-inflammatory therapy.

Oleanolic acid is a natural triterpenoid that belongs to the pentacyclic triterpene class. It is widely found in various plant sources, including olive oil and garlic, and certain medicinal herbs, such as olive (*Olea europaea*), hawthorn (*Crataegus* spp.), and Chinese privet (*Ligustrum lucidum*)[11]. As a biologically active compound, oleanolic acid has gained significant attention from researchers and the pharmaceutical industry owing to its diverse and promising medicinal properties. It also exhibited potent anti-inflammatory, antioxidant, and hepatoprotective effects[12]. In addition, it has shown potential as an antiviral, antimicrobial, and anticancer agent[13]. However, the mechanisms underlying the anti-inflammatory effects of oleanolic acid remain unknown and require further investigation.

This study aimed to identify a novel activator of SHP2 and assess its anti-inflammatory activity. Our results demonstrated that oleanolic acid directly binds to activated SHP2, preserving its open conformation, and resulting in sustained but low-level SHP2 activation. This led to the suppression of inflammatory responses by inhibiting STAT3 phosphorylation and Th17 differentiation. Overall, our findings suggest that preserving SHP2 activity with oleanolic acid can selectively inhibit STAT3 signaling, offering promise for mitigating Th17-mediated inflammation.

2. Material and methods

2.1. Regents

Mouse CD4 (L3T4) MicroBeads were purchased from Miltenyi Biotec (Bergisch Gladbach, Germany). 2,4,6-Trinitrobenzene sulfonic acid (TNBS), 6,8-difluoro-4-methylumbelliferyl phosphate (DiFMUP), Tris (2-carboxyethyl)phosphine (TCEP), sodium deoxycholate, Con A, proteinase K and dexamethasone were purchased from Sigma−Aldrich (St. Louis, MO, USA). Recombinant cytokines, including IL-12, IL-4, IL-6, TGF-β, IL-2, and IFN-γ, were purchased from R&D Systems (Minneapolis, MN, USA). Oleanolic acid and SHP099 were purchased from MedChemExpress (USA). Anti-STAT1, anti-STAT3, phospho-STAT (including phospho-STAT1 and 3) Ab sampler kit, and anti-pY580-SHP-2 were purchased from Cell Signaling Technology (Beverly, MA, USA). Anti-CD3, anti-CD28, anti-IFN-γ mAb, anti-IL-12 mAb, anti-IL-4 mAb, anti-CD4-FITC, anti-CD4-PE, anti-CD4-BV421, anti-CD25-APC, anti-IL-4-APC, anti-Foxp3-PE, anti-IFN-γ-APC, anti-IFN-γ-PE, anti-IL-17A-APC, anti-IL-17A-FITC, and anti-IL-17A-PE were purchased from BD Pharmingen (San Diego, CA, USA). Anti-actin, anti-SHP-2, anti-GAPDH, and anti-E-cadherin were purchased from Santa Cruz Biotechnology (Santa Cruz, CA, USA).

2.2. Mice

Six-to eight-week-old female C57BL/6 mice were purchased from GemPharmatech Co., Ltd. (Nanjing, China). Animal welfare and experimental procedures were performed in strict accordance with the Guide for the Care and Use of Laboratory Animals (National

Institutes of Health, USA) and approved by the Animal Care and Use Committee of Nanjing University (Nanjing, China). All efforts were made to minimize animals' suffering and to reduce the number of animals used.

2.3. Naive $CD4^+$ Th1, Th17, and regulatory T cell differentiation in vitro

Naive $CD4^+$ T cells were purified from mice with MicroBeads and differentiated *in vitro*. For Th1, Th17, and regulatory T cell (T_{reg}) differentiation, naive $CD4^+$ T cells were incubated with plate-bound mAbs of anti-CD3 and anti-CD28 under Th1 conditions (10 ng/mL IL-12, 1 μg/mL anti-IL-4 mAb), Th17 conditions (1 μ g/mL anti-IL-4 mAb, 10 μg/mL anti-IFN-γ mAb, 20 ng/mL IL-6, 1 ng/mL TGF-β), or T_{reg} conditions (1 ng/mL TGF-β, 50 U/mL IL-2) for 72 h. Differentiated Th cells were washed and applied to intracellular staining and flow cytometry.

2.4. Induction of TNBS-induced colitis in mice and drug administration

Murine colitis was induced by TNBS following a published protocol with some modifications. Briefly, adult male C57BL/6 mice were sensitized with 150 μL 1% TNBS solution on abdominal skin 7 days before the challenge. On the challenge day, mice were lightly anesthetized, and TNBS solution (2.5 mg TNBS in 50% ethanol solution) was administered intrarectally. Sham control mice received 50% ethanol only. Daily monitoring for body weight loss and survival was conducted. On Days 0, 1, and 2, mice were orally administered with 10 or 30 mg/kg of oleanolic acid or intraperitoneally injected with 0.5 mg/kg of dexamethasone in PBS. In another experiment, Mice received oral administration of 10 mg/kg of oleanolic acid alone, 10 mg/kg of oleanolic acid combined with 5 mg/kg of SHP099, or 5 mg/kg of SHP099 in PBS. Control mice were given PBS alone.

2.5. Cytokine analysis by enzyme-linked immunosorbent assay (ELISA)

The levels of IL-1β, IL-6, IFN-γ, IL-17A, and TNF-α in the colonic tissue were quantified using ELISA kits (Dakewe, Beijing, China).

2.6. Immunofluorescence (IF) and immunohistochemistry (IHC)

IF and IHC on paraffin-embedded tissue sections were performed as reported[14]. Briefly, cells or tissue sections were fixed in 4% formaldehyde, permeabilized in 0.05% TritonX-100 in PBS or saponin (Beyotime), and incubated in a blocking solution containing 3% goat serum. For IF, samples were stained with primary antibodies at 4 °C overnight, followed by incubation with fluorescently labeled secondary antibodies. Coverslips were mounted in an antifade solution containing DAPI and imaged using a confocal laser scanning microscope or fluorescence microscope. For IHC, sections were incubated with specific primary antibodies for 2 h at room temperature, then incubated with streptavidin-HRP for 40 min, stained using DAB substrate, and counter-stained with hematoxylin. Images were acquired using a microscope (Olympus). Histological evaluation of hematoxylin and eosin (H&E)-stained colonic sections was graded in a blinded manner as described[15].

2.7. Western blotting

Proteins were extracted using lysis buffer, separated by SDS−polyacrylamide gel electrophoresis, and then transferred onto polyvinylidene difluoride membranes. The membranes were subsequently incubated overnight at 4 °C with primary antibodies, followed by incubation with a horseradish peroxidase-coupled secondary antibody. Protein detection was accomplished using the Lumi-GLO chemiluminescent substrate system.

2.8. Protein expression and purification

The DNA sequence encoding recombinant full-length SHP2-WT or SHP2-E76K lacking the C-terminal tail (residues 1−525) was sub-cloned into the pET-15b expression vector containing a 6 × His-tag. Then protein was expressed in *Escherichia coli* BL21 (DE3) and purified by affinity chromatography with Ni-NTA beads (Changzhou Smart-Lifesciences Biotechnology Co., Ltd.). Subsequently, the components containing target protein were collected, concentrated, and further purified by size exclusion chromatography on a Superdex 75 Increase 10/300 GL column (GE Healthcare) and exchanged into MST buffer (25 mmol/L HEPES pH 7.5, 100 mmol/L NaCl, 2 mmol/L TCEP).

2.9. Protein thermal stability analysis

The protein thermal shift assay was performed according to the Protein Thermal Shift™ Dye Kit's (ThermoFisher Scientific) instruction. Briefly, 3 μg SHP2-WT or SHP2-E76K per well was mixed with 30 μmol/L compounds or not, then the diluted Protein Thermal Shift™ Dye was added to each well and all samples were placed on ice for 30 min. These samples were applied to Applied Biosystems® for melting curve and the data analysis was performed on Protein Thermal Shift™ software.

2.10. Phosphatase activity assay in vitro

The phosphatase activity assay was conducted in 96-well black polystyrene plates at room temperature, with a final reaction volume of 100 μL and the following buffer conditions: 60 mmol/L HEPES, pH 7.2, 75 mmol/L NaCl, 75 mmol/L KCl, 1 mmol/L EDTA, 0.1% TritonX-100, 1 mmol/L TECP. The catalytic activity of SHP2 was monitored using the surrogate substrate DiFMUP in a prompt fluorescence assay. 0.5 nmol/L SHP2-WT was incubated with 30 μmol/L compounds for 30 min, then the surrogate substrate DiFMUP was added to the reactions and incubated for 25 min. The reactions were then stopped by adding 5 μL 160 μmol/L solution of bpV (Phen). The fluorescence signal was monitored using a microplate reader (M200PRO), and the excitation and emission wavelengths were 340 and 450 nm, respectively[16].

2.11. Intracellular phosphatase activity assay

T cells isolated from spleens of normal female mice were cultured in 6-well plates at 2×10^6/well and treated either with or without 3, 10, or 30 μmol/L oleanolic acid for 1 h. Cells were collected and lysed using cell lysis buffer for Western and IP (Beyotime). The supernatants were obtained by centrifugation, and protein concentrations of each sample were determined with the Pierce BCA Protein Assay kit (ThermoFisher Scientific) and diluted to 1 mg/mL. Each sample was divided into two parts, with one part

treated with 10 μmol/L SHP099 while another was not. The phosphatase activity of both parts was examined in the same way as the phosphatase activity assay *in vitro*, and the activity of SHP2 was considered by subtracting the fluorescence intensity of the two parts. Finally, the normalized activity of SHP2 of each group was calculated based on the subtraction of fluorescence intensity in each group.

2.12. Microscale thermophoresis (MST)

Buffer exchange and fluorescent dye labeling were performed on 10 μmol/L full-length SHP2-WT or SHP2-E76K according to the Monolith™ RED-NHS Next-Generation Protein Labeling Kit. The diluted oleanolic acid (16 concentration gradients) were respectively mixed with the equal volume labeled protein and incubated for 10 min at room temperature[17]. MST assays were subsequently performed using a Monolith NT.115 (Nano Temper). MO. Affinity analysis software was used for the combined analysis.

2.13. Limited proteolysis−mass spectrometry (LiP-MS) assay

LiP-MS assay was performed as reported previously[18]. Briefly, samples containing 120 μg of purified recombinant SHP2 were treated with 30 μmol/L oleanolic acid or not at room temperature for 10 min. Proteinase K was added simultaneously to all the samples at a proteinase K to substrate mass ratio of 1:100 and incubated at room temperature for 5 min. Digestion reactions were stopped by heating samples for 3 min at 98 °C followed by the addition of sodium deoxycholate to a final concentration of 5%. Samples were then heated again at 98 °C for 3 min. Protein fragments from the proteinase K cleavage step were reduced with 5 mmol/L TCEP for 40 min at 37 °C and then alkylated by incubating 30 min at 25 °C with 20 mmol/L iodoacetamide in the dark. Samples were diluted with 0.1 mol/L ammonium bicarbonate to a final concentration of 1% sodium deoxycholate. Finally, all the samples were subjected to mass spectrometry assay by ChomiX Biotech (Nanjing) Co., Ltd.

2.14. Intracellular staining

After completing the differentiation of $CD4^+$ T cells, the cells were treated with Cell Stimulation Cocktail (supplemented with protein transport inhibitors, 500 × concentration, ThermoFisher Scientific). Subsequently, the cells were harvested and suspended in 100 μL of anti-CD4-FITC antibody, followed by a 15-min incubation at 4 °C. The cells were then washed twice with 1 × PBS and resuspended in 1 × Fixation/Permeabilization buffer (ThermoFisher Scientific) for 20 min at 4 °C. Following fixation, the cells were washed once with 1 × PBS before adding 1 × permeabilization buffer (ThermoFisher Scientific) containing anti-IFN-γ-APC and anti-IL-17A-PE (or anti-IL4-APC and anti-Foxp3-PE) and incubating at 4 °C for 30 min. After staining, the cells were resuspended in 500 μL of 1 × PBS, and FACS analysis was performed using an Attune NxT Cytometer (ThermoFisher Scientific).

2.15. Statistical analysis

The results are expressed as the mean ± standard error of mean (SEM) of three independent experiments and each experiment included triplicate sets. Data were statistically evaluated by one-way ANOVA followed using Dunnett's test between the control group and multiple-dose groups. The level of significance was set at a P value of 0.05.

3. Results

3.1. Oleanolic acid directly binds to activated SHP2 and prevented its deactivation by SHP099

To identify phosphatase activators of SHP2 that could maintain its open conformation, we performed a two-step screening assay using SHP2-E76K (1−525), an active open-state mutant of SHP2. Protein thermal shift technology was used in primary screening to obtain compounds that stabilized SHP2-E76K. The impact of the targeted compounds on SHP099 IC_{50} was detected using an *in vitro* phosphatase assay for secondary screening (Fig. 1A). Fourteen candidates were selected from 1900 FDA-approved and 30 of our own SE series compounds in primary screening for the SHP099 IC_{50} assay, and oleanolic acid exhibited the best effect (Fig. 1B and C). First, to confirm whether oleanolic acid activated SHP2 by maintaining its active open state, the interaction between oleanolic acid and SHP2 was evaluated. Oleanolic acid treatment elevated the melting point of SHP2-E76K in a dose-dependent manner, thereby suggesting that oleanolic acid stabilized the conformation of SHP2-E76K (Fig. 1D). The dissociation constant between SHP2-WT and SHP2-E76K and oleanolic acid measured by MST was 7.3 and 3.0 μmol/L, respectively. This suggests that oleanolic acid may have a higher affinity for binding to activated SHP2 (Fig. 1E). Under 30 μmol/L oleanolic acid treatment, the IC_{50} of SHP099 was observed to be 10 times higher than that of the control group (Fig. 1F). Additionally, the intracellular phosphatase activity of SHP2 in T cells increased by approximately 40% after being treated with 30 μmol/L oleanolic acid (Fig. 1G). To assess the selectivity of oleanolic acid for protein tyrosine phosphatases (PTPs), we investigated its effects on two homologous family members of SHP2, PTP1B and SHP1. The results revealed that while oleanolic acid slightly inhibited PTP1B activity, it did not affect SHP1 activity (Supporting Information Fig. S1). To determine the primary binding sites of oleanolic acid and SHP2, LiP-MS experiments were performed as described in the previous study[18] (Fig. 1H). The binding of oleanolic acid prevented cleavage by the protease K, leading to the emergence of a long peptide and a decrease of two short peptides under 30 μmol/L oleanolic acid treatment, thus suggesting oleanolic acid might bind to the long peptide and protect it from protease K digestion (Fig. 1I). Based on the LiP-MS results, a binding model of SHP2 to oleanolic acid was predicted using macromolecular docking, and the interactions between oleanolic acid and the PTP domain of SHP2 were visualized using PyMol (Fig. 1J and K). Macromolecular docking results revealed that oleanolic acid bound to the amino acid residues R362, K364, and K366 in the active center of the activated SHP2 and occupied the interface between N-SH2 and PTP domain, thereby leading to the disruption of the auto-inhibited state and sustained activation. When R362 was replaced by glutamate, the binding affinity between SHP2 and oleanolic acid significantly decreased, which verified our docking result (Fig. 1L−N).

3.2. Oleanolic acid inhibited phosphorylation of STAT3 and differentiation of Th17

$CD4^+$ T cells are classified into subgroups such as Th1, Th2, Th17, and regulatory T cells (T_{reg}) depending on cell differentiation and functional properties[19]. Th1 and Th17 cells are the two main

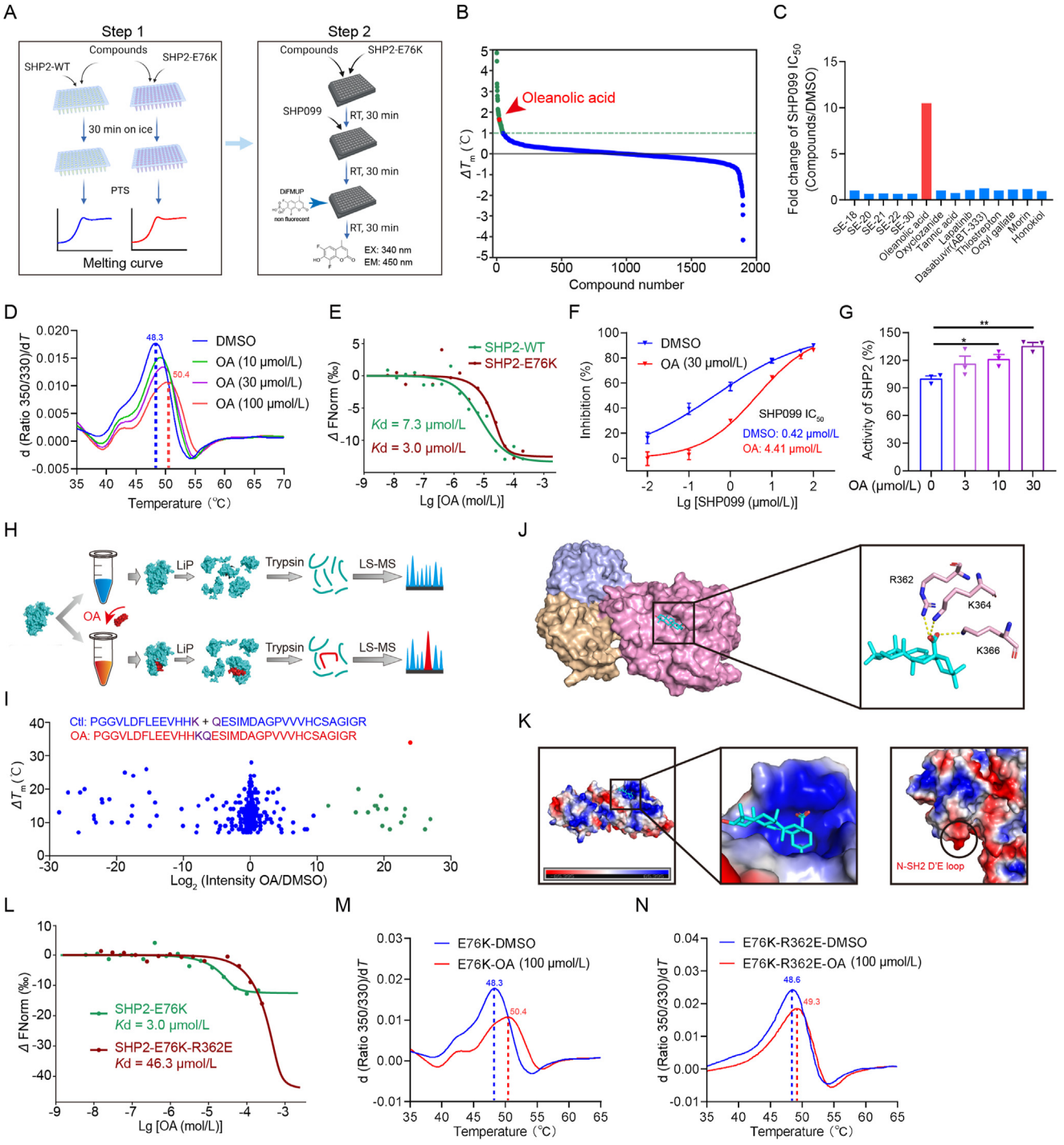

Figure 1 Oleanolic acid directly binds to activated SHP2 and prevents its deactivation by SHP099. (A) Two-step screening strategy for SHP2 activator. Step 1: protein thermal shift (PTS) assay. Step 2: *in vitro* phosphatase assay for examination of the targeted compounds' impact on IC_{50} of SHP099. (B) Primary screening results of more than 1900 FDA-approved drugs and our own SE series compounds. (C) Compounds selected from primary screening, whose $\Delta T_m > 1$ °C, were subjected to step 2 examination. (D) Protein thermal stability analysis was performed to examine the effect of oleanolic acid on SHP2-E76K. (E) The interaction of SHP2-E76K and SHP2-WT with oleanolic acid was determined using MST, respectively. (F) IC_{50} of SHP099 was examined *via in vitro* phosphatase assay (blue: DMSO, red: oleanolic acid) ($n = 3$). (G) After treatment with 30 μmol/L oleanolic acid, cellular SHP2 activity of mouse spleen T cells was measured ($n = 3$). (H, I) SHP2-E76K was treated or not with oleanolic acid. A limited proteolysis step is performed with proteinase K under native conditions, followed by complete digestion with trypsin under denaturing conditions to generate MS-measurable peptides. (J) The binding model of SHP2-E76K and oleanolic acid was predicted by macromolecular docking according to the result of the LiP-SMap experiment and surface electrostatic potential of SHP2-E76K−OA complex was exhibited. (K) Surface electrostatic potential of SHP2. (L) The interaction of SHP2-E76K-R362E with oleanolic acid was determined using MST. (M, N) Protein thermal stability analysis was performed to examine the effect of oleanolic acid on SHP2-E76K-R362E. Values are shown as the mean ± SEM of three independent experiments. $^*P < 0.05$, $^{**}P < 0.01$ *vs* as indicated.

pro-inflammatory subgroups owing to their secretion of IFN-γ and IL-17, respectively[20], while regulatory T cells play a vital role in immunosuppression *via* IL-10[21]. Previous studies have shown that Th1 and Th17 cells participated in and aggravated the development of inflammatory bowel diseases[22,23]. The IFN-γ/STAT1 and IL-6/STAT3 pathways were important for Th1 and Th17 T cell differentiation, which were both crucial for inflammatory diseases[24]. Under IL-6 stimulation, STAT3 was recruited to the activated IL-6Rα and phosphorylated at Tyr705. Then, phosphorylated STAT3 homodimerized and was translocated to nuclei, where the homodimer initiated the transcription factor RORγt, indispensable for Th17 differentiation[25]. The role of IFN-γ and STAT1 in Th1 differentiation was similar[26]. Our previous study has demonstrated that fusaruside[22], a small molecule activator of SHP2, inhibited the STAT1−Th1 axis and ameliorated mouse experimental colitis. Therefore, T cells were chosen as the target cells of oleanolic acid in this study and the effect of oleanolic acid on these pathways and T cell differentiation were examined. Our results showed that oleanolic acid increased the intracellular phosphatase activity of SHP2 in T cells. To further validate this observation, p-SHP2 levels in T cells treated with oleanolic acid were examined using Western blot. The results showed that the p-SHP2 level in T cells was the highest 1 h after being treated with 30 μmol/L oleanolic acid (Fig. 2A) and that the level increased in a dose-dependent manner when treated with various concentrations of oleanolic acid (Fig. 2B). IL-6 stimulation resulted in STAT3 activation, whereas oleanolic acid pretreatment inhibited STAT3 activation in a dose-dependent manner (Fig. 2C), while IFN-γ-stimulated p-STAT1 was not altered (Supporting Information Fig. S2A). Furthermore, the effect of oleanolic acid on T cell differentiation was detected using flow

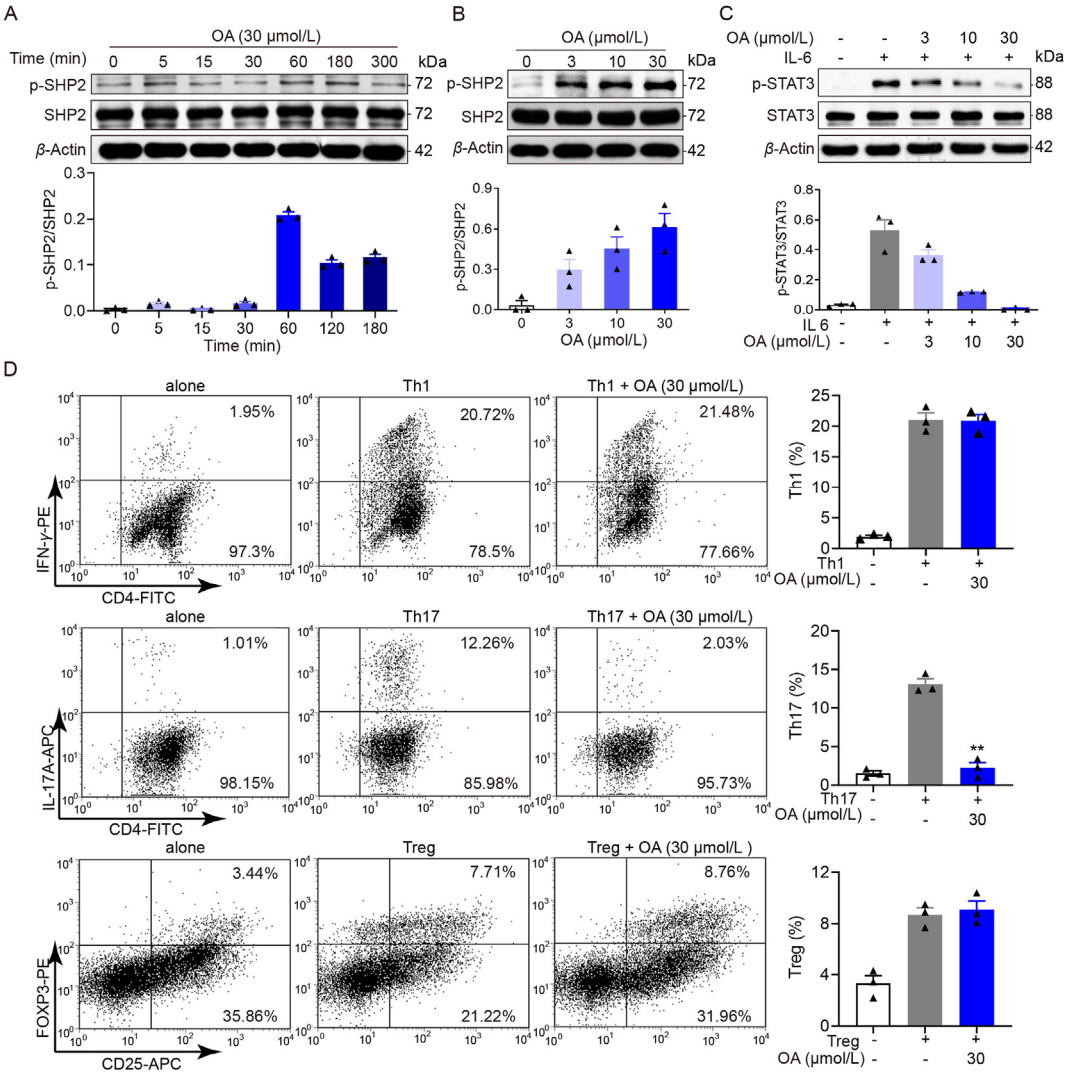

Figure 2 Oleanolic acid selectively inhibited phosphorylation of STAT3 and differentiation of Th17. (A, B) Naive T cells from mice were treated with 30 μmol/L oleanolic acid for different hours or various concentrations for 1 h. Protein levels were assessed by Western blot ($n = 3$). (C) Naive T cells from mice were treated with oleanolic acid, followed by stimulation of IL-6 (25 ng/mL) for 30 min. Protein levels were assessed by Western blot ($n = 3$). (D) Naive $CD4^+$ T cells were purified from mice with MicroBeads and differentiated *in vitro*. Naive $CD4^+$ T cells were incubated with anti-CD3 and anti-CD28 under Th1 conditions, Th17 conditions, or T_{reg} conditions with or without OA (30 μmol/L) for 72 h. Then cells were assessed by FACS ($n = 3$). Values are shown as the mean ± SEM of three independent experiments. $^{**}P < 0.01$ *vs* as indicated.

cytometry, considering the relationship between STAT3 phosphorylation and Th17 differentiation. The differentiation of Th17 cells was markedly suppressed by oleanolic acid, whereas the differentiation of Th1 and T_{reg} cells was insensitive to oleanolic acid treatment (Fig. 2D). Hence, oleanolic acid may suppress the differentiation of Th17 cells by activating tyrosine phosphatase SHP2 and causing the dephosphorylation of STAT3.

3.3. Oleanolic acid-induced interaction between SHP2 and STAT3 blocked recruitment of STAT3 to IL-6R during IL-6/STAT3 signaling

Next, the association between OA-induced SHP2 activation and STAT3-mediated signaling was examined. IL-6Rα was detected in an anti-STAT3 antibody immunoprecipitated protein of IL6-treated T cells, thus indicating that STAT3 was recruited onto the receptor. However, when simultaneously treated with oleanolic acid, the receptor protein was almost undetectable and the level of p-STAT3 decreased in parallel (Fig. 3A). In addition, the phosphorylation of SHP2 in anti-STAT3 immunoprecipitated proteins was considerably reduced after treatment with SHP099 (Fig. 3B), and the inhibitory effect of oleanolic acid on p-STAT3 levels was abolished by SHP099 pretreatment (Fig. 3C). As expected, SHP099 reversed the OA-induced inhibition of recruitment of STAT3 to IL-6R in a dose-dependent manner (Fig. 3D). Immunofluorescence analysis confirmed that oleanolic acid blocks STAT3's transfer to the nuclei. There was a clear reduction in the intensity of the fluorescent signal (red) in the nuclei of T cells treated with oleanolic acid, which corresponded to the oleanolic acid-induced dephosphorylation of STAT3 (Fig. 3E). Thus, these data suggest that p-SHP2 induced by oleanolic acid sequestrates STAT3 from activation, which selectively regulates STAT3 signaling.

3.4. Oleanolic acid ameliorated TNBS-induced experimental colitis in mice

Given the inhibitory effect of oleanolic acid on IL-6-induced STAT3 activation and Th17 differentiation, a TNBS-induced experimental colitis mouse model was used to evaluate the anti-inflammatory capacity. As demonstrated by the changes in body weight, treatment with 30 mg/kg oleanolic acid significantly reversed weight loss to a greater extent than that in the positive control group treated with 0.5 mg/kg dexamethasone (Fig. 4A). Significant attenuation of colon damage was observed in the colons of mice treated with either 10 or 30 mg/kg oleanolic acid or 0.5 mg/kg dexamethasone (Fig. 4B and C). Mesenteric lymph node (MLN) cells were collected, stained and subjected to flow cytometry to measure the differentiation of Th17 and Th1 cells, which demonstrated oleanolic acid suppressed Th17 differentiation (Fig. 4D). Histological analysis indicated that damage to the colonic epithelium was prominently ameliorated by the administration of 10 and 30 mg/kg oleanolic acid or 0.5 mg/kg dexamethasone (Fig. 4E). The expression of E-cadherin was examined by immunohistochemistry, and the results showed that oleanolic acid restored the integrity of adherent junctions destroyed by TNBS (Fig. 4F). Additionally, immunofluorescence histochemistry revealed a significant decrease in the infiltration of $CD4^+$ T cells into the colon tissues of mice treated with oleanolic acid compared to that in the TNBS-treated mice (Fig. 4G). Collectively, these findings demonstrate that oleanolic acid effectively alleviates TNBS-induced experimental colitis in mice.

3.5. SHP2 inhibitor reversed the improvement effect of oleanolic acid on colitis

To verify that the improvement in TNBS-induced colitis by oleanolic acid was dependent on SHP2, the effect of oleanolic acid combined with SHP099, a specific allosteric inhibitor of SHP2, on TNBS-induced colitis was examined. The changes in body weight (Fig. 5A) and colon length (Fig. 5B and C) showed that SHP099 eliminated the ameliorative effect of oleanolic acid on TNBS-induced colitis, thus indicating that the amelioration of TNBS-induced experimental colitis in mice by oleanolic acid was dependent on SHP2. Intracellular staining of MLN cells indicated that SHP099 reversed the OA-inhibited Th17 differentiation (Fig. 5D). To further support this finding, histological analysis, immunohistochemistry, and immunofluorescence were used to examine the macroscopic damage to colonic tissues, integrity of adherent junctions, and infiltration of $CD4^+$ T cells, respectively (Fig. 5E–G). These results further support the finding that oleanolic acid relies on SHP2 to ameliorate colitis.

3.6. Oleanolic acid and stattic had no synergic effect on TNBS-induced mice colitis

To confirm the improving effect of oleanolic acid on colitis was dependent on the STAT3–Th17 pathway, 10 mg/kg of oleanolic acid in combination with 10 mg/kg of stattic, an inhibitor of STAT3, was used in the TNBS-induced mice colitis. As expected, the changes in body weight, colon length, and colon permeability indicated that oleanolic acid and stattic both ameliorated the TNBS-induced mice colitis but they didn't have a significant synergic effect. (Supporting Information Fig. S3A–S3D). Oleanolic acid and stattic both suppressed the differentiation of Th17, while the combination of them did not exhibit a better effect (Fig. S3E). Histological analysis, immunohistochemistry, and immunofluorescence of $CD4^+$ T cell infiltration further demonstrated the improving effect of oleanolic acid on colitis was dependent on STAT3 (Fig. S3F–S3H).

3.7. SHP2 knockout in T cells aggravated TNBS-induced colitis

To investigate the role of SHP2 in $CD4^+$ T cells in colitis, a TNBS-induced colitis mouse model was established using $SHP2^{CD4-/-}$ mice and their WT littermates. The body weight of the mice was recorded daily after being treated with TNBS, and the colon length was measured after sacrificing the mice on the 4th day. $SHP2^{CD4-/-}$ mice exhibited more remarkable body weight loss (Fig. 6A) and a shorter colon length than WT mice (Fig. 6B and C). Serum FD4 concentration was measured, and the results indicated that SHP2 knockout in $CD4^+$ T cells exacerbated the inflammatory responses in the colon induced by TNBS (Fig. 6D). Furthermore, pro-inflammatory cytokine levels in $SHP2^{CD4-/-}$ mice colonic tissues after TNBS challenge increased more prominently than those in WT mice colonic tissues (Fig. 6E and F). Loss of crypts and goblet cells, infiltration of mononuclear cells, and mucosal damage in the colon specimens were relatively severe in $SHP2^{CD4-/-}$ mice, as observed using histological analysis (Fig. 6G). SHP2 knockout in $CD4^+$ T cells promoted $CD4^+$ T cell infiltration into colonic tissues (Fig. 6H). These results demonstrate that SHP2 knockout in $CD4^+$ T cells aggravates TNBS-induced colitis by promoting the production of proinflammatory cytokines.

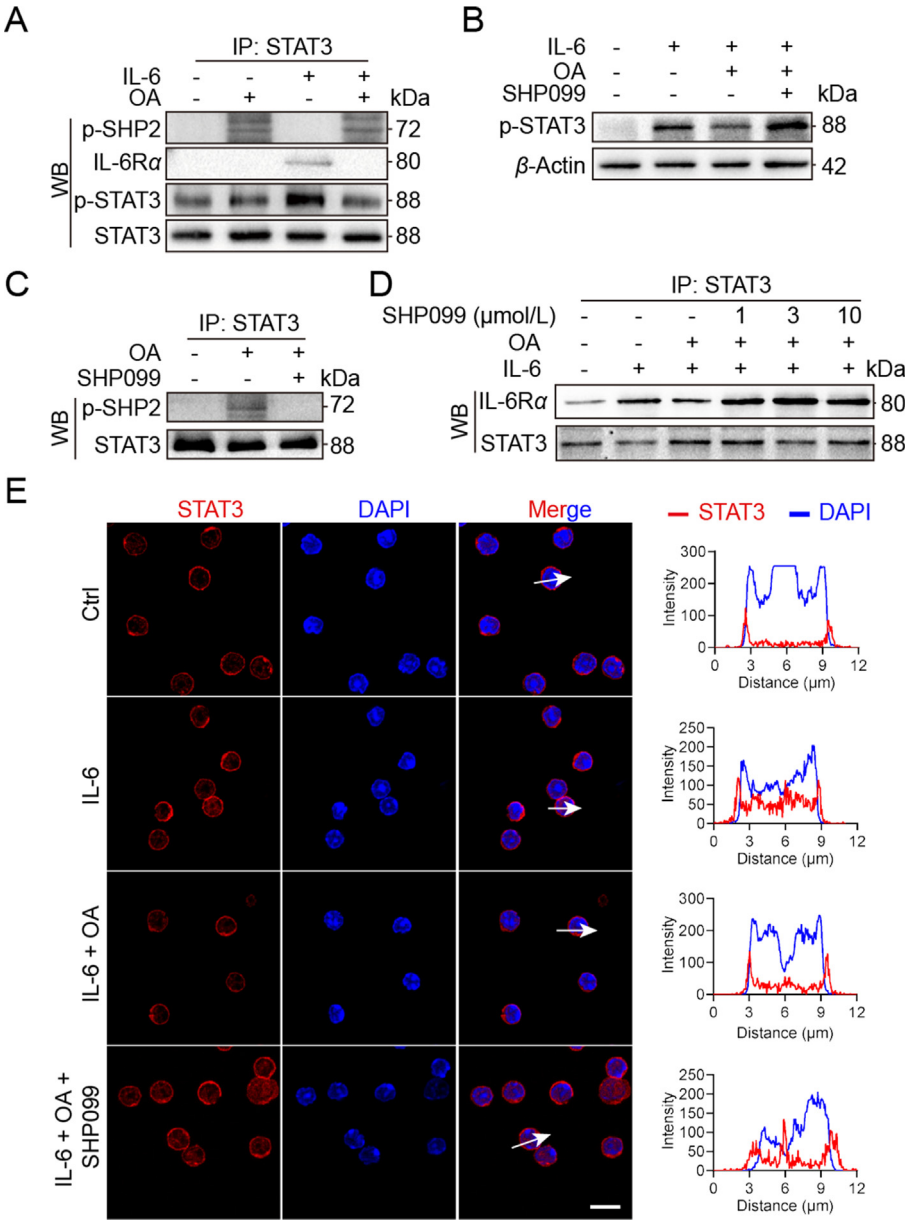

Figure 3 The oleanolic acid-induced interaction between SHP2 and STAT3 blocks recruitment of STAT3 to IL-6R during IL-6/STAT3 signaling. (A) Lymph node-derived T cells were treated or not with 30 μmol/L oleanolic acid for 6 h, and the T cells were then treated with 25 ng/mL of IL-6 for 30 min. After incubation, the total protein was immunoprecipitated with an Ab against STAT3. The immunoprecipitants were assessed by Western blotting. (B, C) Lymph node-derived T cells were treated with 30 μmol/L oleanolic acid with or without SHP099 for 6 h. The cell extracts were then subjected to co-immunoprecipitation or Western blot analysis. (D) After being treated with 1, 3, or 10 μmol/L SHP099 for 24 h and followed by 30 μmol/L OA for 1 h and 25 ng/mL of IL-6 for 30 min, the effect of SHP099 on oleanolic acid-regulated recruitment of STAT3 to IL-6R was detected by co-immunoprecipitation. (E) Lymph node-derived T cells were treated with or without 30 μmol/L oleanolic acid for 6 h, and the T cells were then treated with 25 ng/mL of IL-6 for 30 min. After treatment, the cells were analyzed by immunofluorescence. The results shown are representative of three independent experiments. Scale bar, 10 μm.

3.8. SHP2 knockout in T cells promoted Th1 and Th17 differentiation in vivo

Differentiation of $CD4^+$ T cells plays a crucial role in regulating inflammatory responses. To evaluate the effect of SHP2 knockout on $CD4^+$ T cell differentiation, flow cytometry and Western blotting were performed. The results demonstrated that SHP2 knockout in $CD4^+$ T cells led to increased Th1 and Th17 differentiation (Fig. 7A and B) and elevated the levels of intracellular p-STAT1 and p-STAT3 in MLN cells (Fig. 7C–F) after TNBS treatment. These findings suggest that SHP2 functions as a negative regulator of inflammatory responses by inhibiting Th1 and Th17 differentiation.

3.9. SHP2 knockout in T cells abolished the improvement effect of oleanolic acid on colitis

To further confirm that the beneficial effects of oleanolic acid on TNBS-induced colitis depend on SHP2, the effect of oleanolic acid on TNBS-induced colitis in $SHP2^{CD4-/-}$ mice was examined.

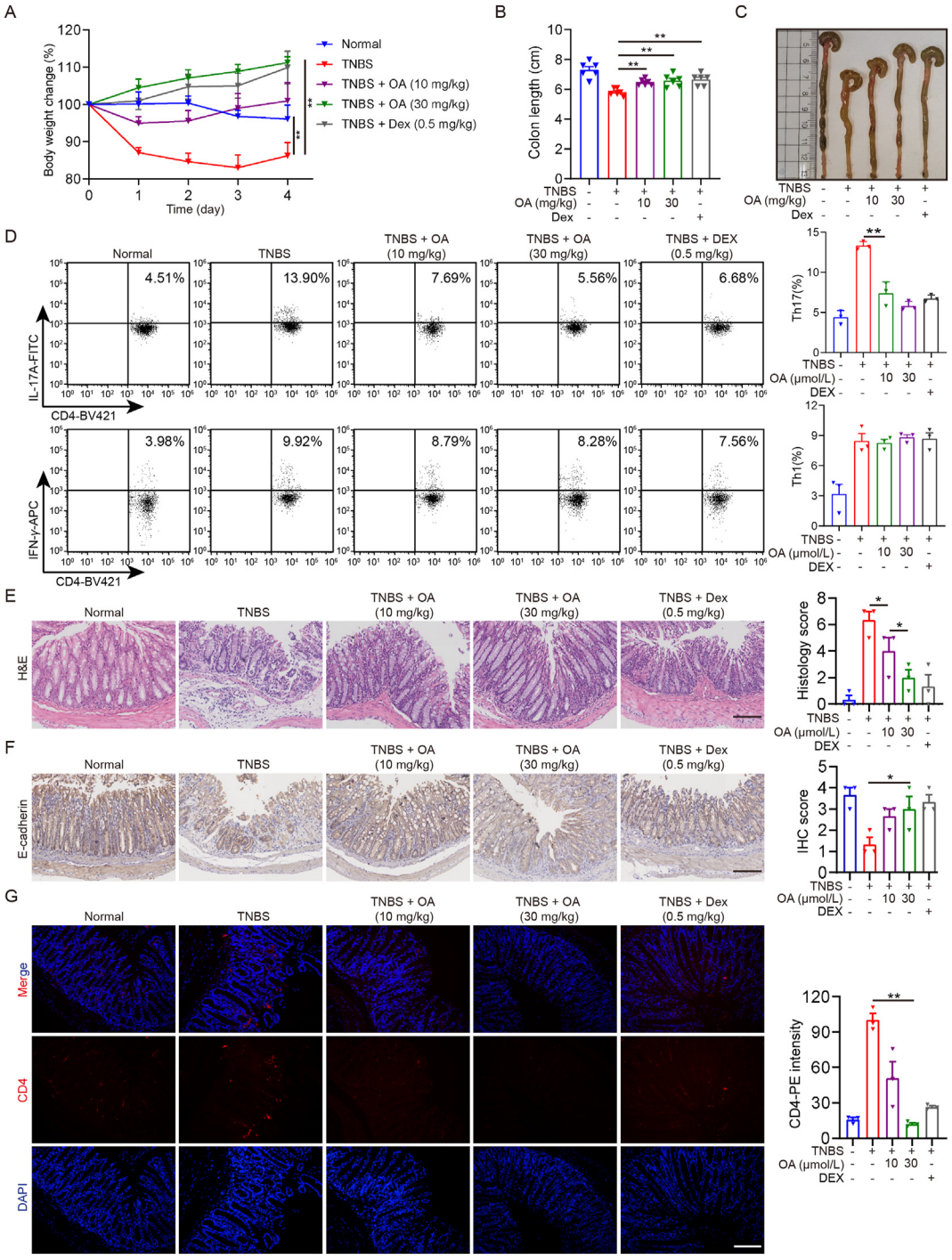

Figure 4 Oleanolic acid ameliorated TNBS-induced experimental colitis in mice. Mice were challenged with TNBS on Day 0, and oral administration of oleanolic acid was carried out from Days 0−4. (A) Body weight was measured daily throughout the experiment ($n = 6$). (B, C) After sacrifice on Day 4, colon damage was evaluated by colon length ($n = 6$). (D) Mesenteric lymph node cells were collected and activated with PMA and ionomycin in the presence of monensin for 4 h. Intracellular IFN-γ and IL-17A production of $CD4^+$ T cells was stained and measured by flow cytometry ($n = 3$). (E) Sections of the colon were collected and stained with H&E ($n = 3$). (F) Colon tissue sections were stained for E-cadherin ($n = 3$). (G) Immunofluorescence histochemistry for $CD4^+$ T cell infiltration ($n = 3$). Values are shown as the mean ± SEM. $^*P < 0.05$, $^{**}P < 0.01$ *vs* as indicated. Dex: dexamethasone. Scale bar, 200 μm.

Changes in the body weight (Fig. 8A) and colon length (Fig. 8B and C) showed that the amelioration of oleanolic acid in TNBS-induced colitis was eliminated in $SHP2^{CD4-/-}$ mice. Additionally, oleanolic acid failed to improve colon permeability in $SHP2^{CD4-/-}$ mice treated with TNBS (Fig. 8D). Flow cytometry analysis of mesenteric lymph node (MLN) cells revealed that SHP2 knockout in $CD4^+$ T cells promoted Th17 differentiation, an effect not reversed by oleanolic acid treatment, indicating the dependency of oleanolic acid's efficacy in TNBS-induced colitis on SHP2 (Fig. 8E). This finding was further supported by the

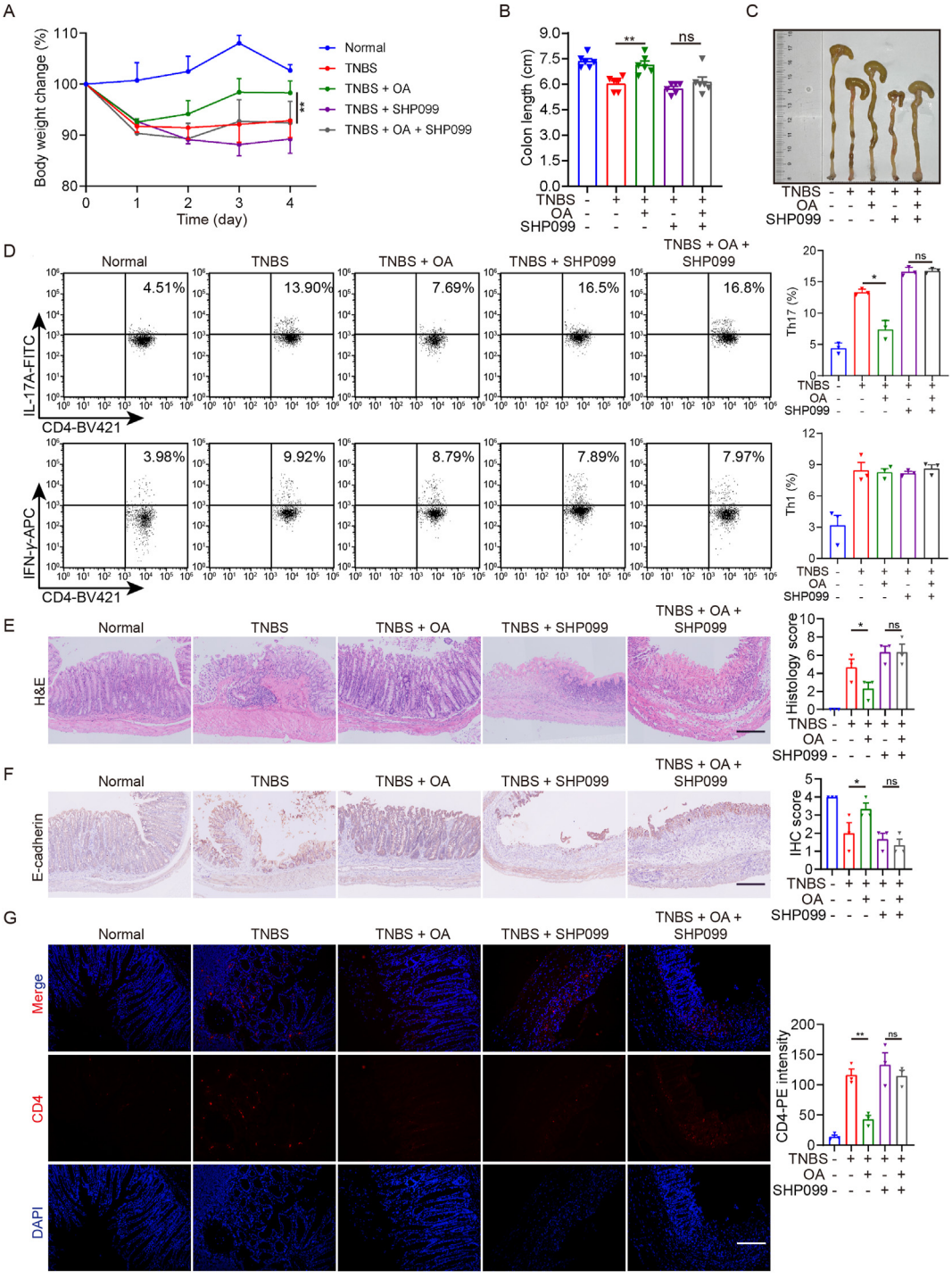

Figure 5 SHP2 inhibitor reversed the improvement of oleanolic acid on colitis. Mice were challenged with TNBS on Day 0, followed by oral administration of oleanolic acid and intraperitoneal injection of SHP099 from Days 0–4, respectively. (A) Body weight was recorded daily throughout the experiment ($n = 6$). (B, C) After sacrifice on Day 4, colon damage was evaluated by colon length ($n = 6$). (D) Mesenteric lymph node cells were collected and activated with PMA and ionomycin in the presence of monensin for 4 h. Intracellular IFN-γ and IL-17A production of $CD4^+$ T cells was stained and measured by flow cytometry ($n = 3$). (E) Sections of the colon were collected and stained with H&E ($n = 3$). (F) Colon tissue sections were stained for E-cadherin ($n = 3$). (G) Immunofluorescence histochemistry for $CD4^+$ T cell infiltration ($n = 3$). Values are shown as the mean ± SEM. $^*P < 0.05$, $^{**}P < 0.01$ *vs* as indicated; ns: no significance. Scale bar, 200 μm.

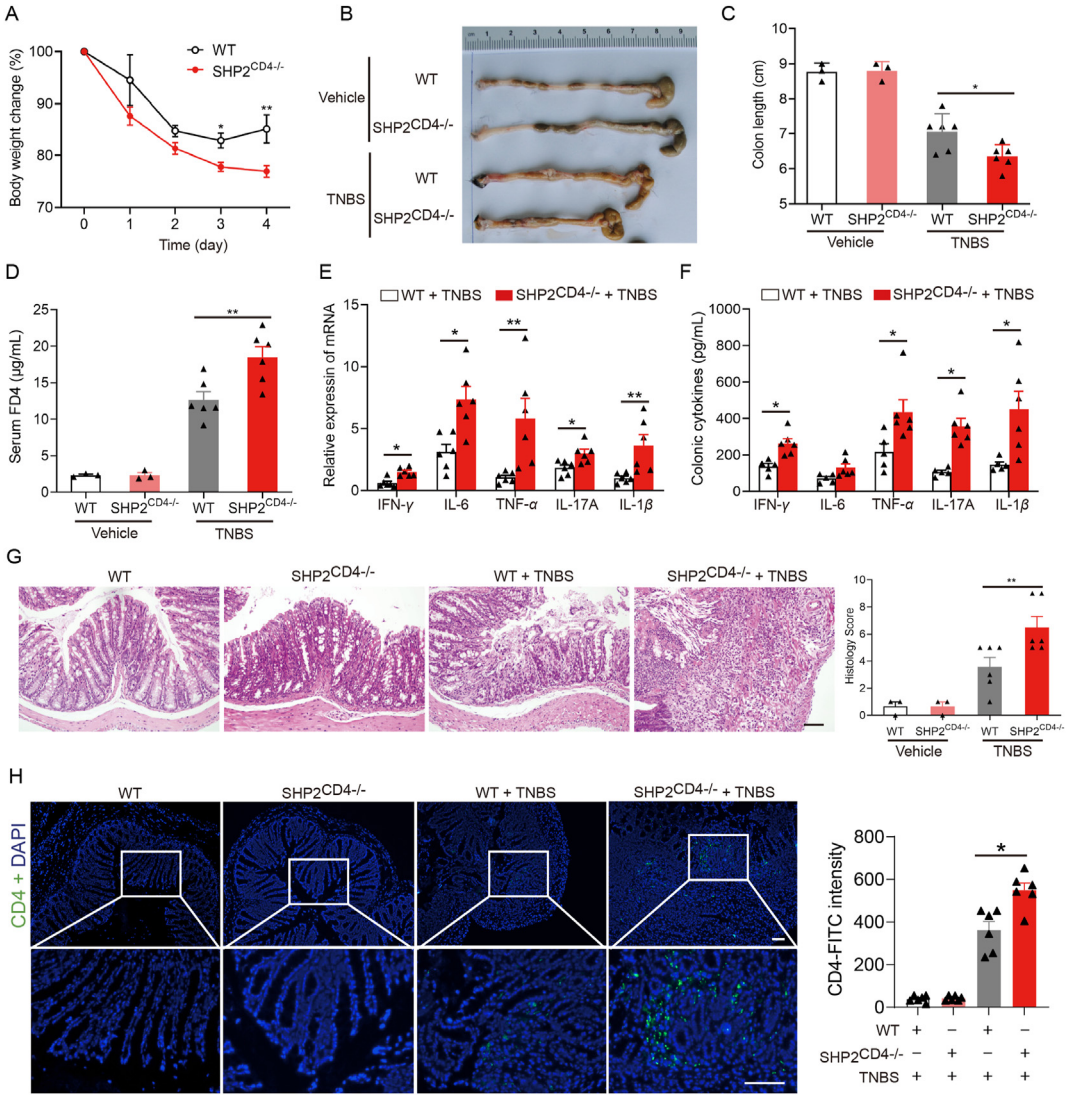

Figure 6 SHP2 knockout in T cells aggregated TNBS-induced colitis. Mice were subjected to TNBS-induced colitis modeling. (A) Change of body weight is expressed as a percentage of the original body weight. (B, C) The gross anatomy of colons and colon length was measured. (D) Quantification of serum FD4 concentration from WT *vs* $SHP2^{CD4-/-}$ mice. (E) The mRNA expressions of inflammation-related cytokines IFN-γ, TNF-α, IL-1β, and IL-17A in colonic tissues were determined by real-time PCR. (F) Protein levels of cytokines including IFN-γ, TNF-α, IL-1β, and IL-17A in colonic homogenate were determined by ELISA. (G) Sections of the colon were collected and stained with H&E. (H) Immunofluorescence histochemistry for $CD4^+$ T cell infiltration. Values are shown as the mean ± SEM of 6 mice. $^*P < 0.05$, $^{**}P < 0.01$ *vs* as indicated. Scale bar, 200 μm.

analysis of the macroscopic damage to colonic tissue, integrity of adherent junctions, and infiltration of $CD4^+$ T cells (Fig. 8F–H).

4. Discussion

In this study, oleanolic acid was identified as a distinctive activator of SHP2. It was observed that oleanolic acid binds to the cleft of the PTP active center of activated SHP2, thereby protecting SHP2 from deactivation. This selective disruption of the STAT3–Th17 axis resulted in the amelioration of TNBS-induced colitis in mice.

SHP2 was initially discovered as a proto-oncoprotein that regulated cell proliferation, growth, and differentiation by activating the MAPK/ERK pathway[27]. Gain-of-function mutations in SHP2, such as SHP2-E76K, increase the risk of cancers, including juvenile myelomonocytic leukemia, acute myeloid leukemia, and some solid cancers[28]. Therefore, SHP2 inhibitors, such as RMC4630 and TNO155, have been widely reported over the last decade for cancer chemotherapy[29]. In comparison, only a few SHP2 activators have been identified. Several studies have revealed that activating SHP2 exhibits excellent pharmacological activities, particularly prominent anti-inflammatory effects[30]. Therefore, it is important to search for activators of SHP2. Although SHP2 activators, such as trichomide A[31], fusaruside[22], and lovastatin[32], have extraordinary pharmacological activities, the mechanisms by which they activate SHP2 have not yet been elucidated. Our findings reveal the mechanisms of activation of SHP2 by oleanolic acid and its anti-inflammatory effects in detail. Furthermore, we proposed that SHP2 can be allosterically activated by maintaining its open conformation, thus providing a novel strategy for identifying SHP2 activators.

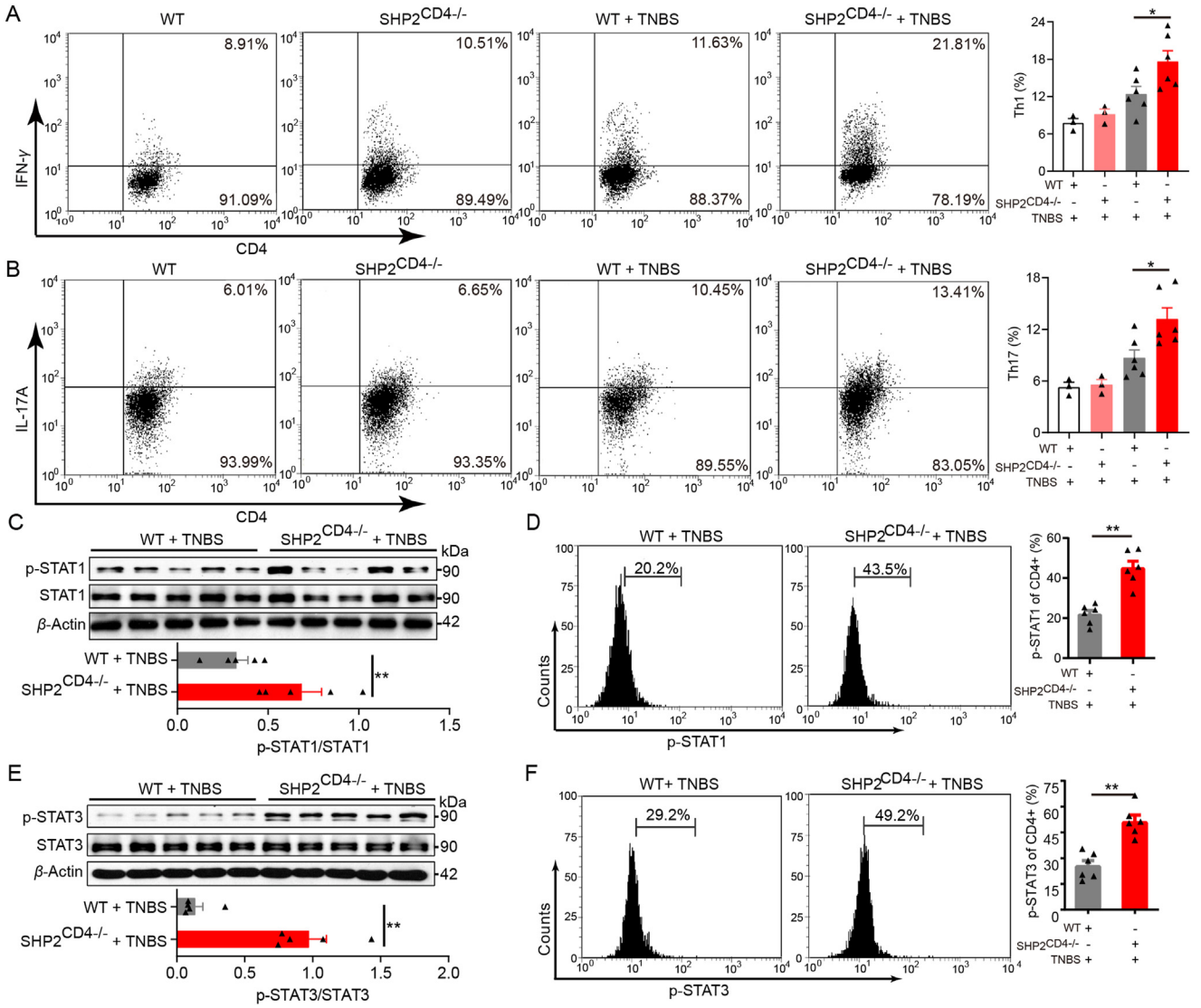

Figure 7 SHP2 knockout in T cells promoted Th1 and Th17 differentiation *in vivo*. (A, B) Mesenteric lymph node (MLN) cells were collected on Day 7 of induction and activated with PMA and ionomycin in the presence of monensin for 4 h. Intracellular IFN-γ and IL-17A production of $CD4^+$ T cells was measured by flow cytometry. (C) Expression of p-STAT1 in MLN cells was examined by Western blot. (D) MLN cells were analyzed for CD4 and intracellular p-STAT1 expression by flow cytometry. The plots were gated on $CD4^+$ T cells, and the percentage of p-STAT1-expressing $CD4^+$ T cells was determined (bar graphs). (E) Expression of p-STAT3 in MLN cells was examined by Western blot. (F) MLN cells were analyzed for CD4 and intracellular p-STAT3 expression by flow cytometry. The plots were gated on $CD4^+$ T cells, and the percentage of p-STAT3-expressing $CD4^+$ T cells was determined (bar graphs). The data represent the mean ± SEM, $n = 6$; $^*P < 0.05$, $^{**}P < 0.01$ *vs* as indicated.

The binding of a phosphotyrosine peptide to tandem SH2 domains opens the closed state, exposes the catalytic cleft, and activates SHP2[33]. It is not feasible to search for direct small-molecule activators that open the auto-inhibited state of SHP2, considering that the activation of SHP2 requires a phosphotyrosine peptide under physiological conditions. Instead, maintaining SHP2 in an activated state is relatively practical. It has been reported that phosphatase PRL-3 promotes IL-6-STAT3 signaling *via* downregulating SHP2 phosphorylation[34]. Therefore, protecting activated SHP2 from phosphatase deactivation is a crucial way to sustain the activity of SHP2, and oleanolic acid is the exact small molecule that matches the required conditions.

Phosphatase SHP2 exhibits a broad spectrum of substrate binding upon activation. Extensive research, including both earlier literature and our study, has corroborated SHP2's ability to bind to diverse substrates such as including STAT1[22], STAT3[34], PD-1[35], ANT1[10], HOOK[36], TLR7[37], PARKIN[32], DOCK1[38]. This binding occurs under varying conditions, such as in the presence of growth factors, PD-L1 signaling, or inflammasome activation. Intriguingly, SHP2 selectively engages with specific substrates in response to distinct inflammatory signals, thereby highlighting the pivotal role of SHP2 substrate selectivity in regulating inflammatory homeostasis. Moreover, this selectivity governs the diverse effects of SHP2 on inflammation and dictates when SHP2 inhibitors or activators are most beneficial. Despite these insights, the mechanisms underlying SHP2's substrate recognition and selective binding remain elusive. In one of our prior investigations, we demonstrated that the small molecule

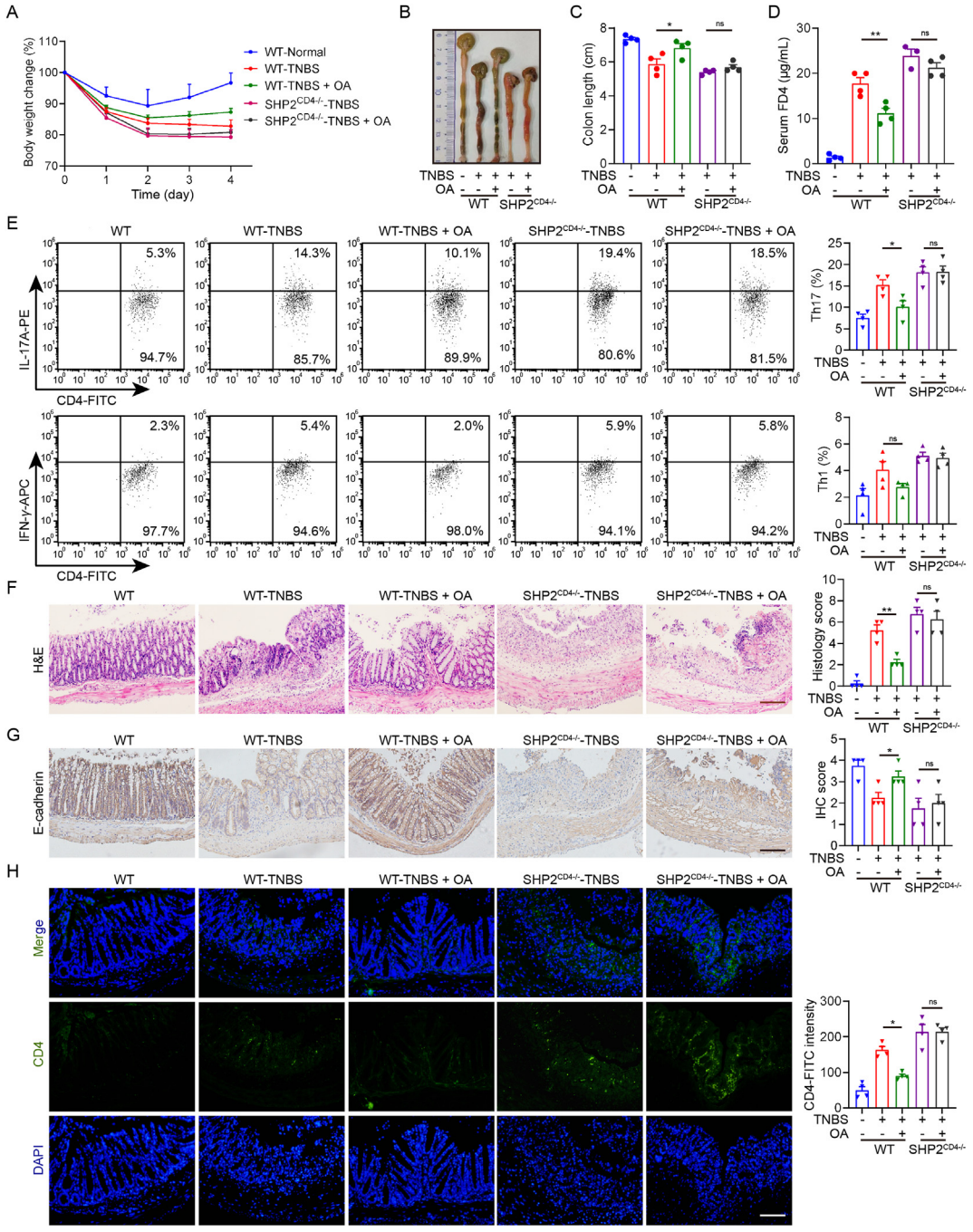

Figure 8 SHP2 knockout in T cells abolished the improvement effect of oleanolic acid on colitis. Mice were challenged with TNBS on Day 0 and orally administered oleanolic acid from Days 0−4. (A) Body weight was measured daily throughout the experiment. (B, C) After sacrifice on Day 4, colon damage was evaluated by colon length. (D) Quantification of serum FD4 concentration. (E) Mesenteric lymph node cells were collected and stimulated with PMA and ionomycin in the presence of monensin for 4 h. Intracellular IFN-γ and IL-17A production of $CD4^+$ T cells was measured by flow cytometry. (F) Sections of the colon were collected and stained with H&E. (G) Colon tissue sections were stained for E-cadherin. (H) Immunofluorescence histochemistry was utilized to evaluate $CD4^+$ T cell infiltration. Values are shown as the mean ± SEM of 4 mice. $^*P < 0.05$, $^{**}P < 0.01$ *vs* as indicated; ns: no significance. Scale bar, 200 μm.

fusaruside could induce an SHP2-mediated selective interaction with STAT1[22]. Notably, fusaruside does not directly activate SHP2, raising intriguing questions about the underlying mechanisms of this selectivity. Additionally, we discovered that OA can bind to SHP2, maintaining its open conformation, albeit weaker than its interaction with substrates. We hypothesize that this weak interaction facilitates SHP2's access to its substrates. It is plausible that the degree of openness in SHP2's conformation may dictate the substrates it interacts with, although further evidence is needed to substantiate this hypothesis. We will undertake a two-pronged approach. Firstly, we plan to screen additional compounds capable of binding to and activating SHP2, ultimately

achieving a higher degree of selective substrate binding. Secondly, we aim to employ a broader array of methods to analyze the conformational changes that occur after SHP2 activation.

Considering the carcinogenicity of gain-of-function mutations in SHP2[39], there may be some controversies regarding SHP2 activators. Interestingly, all reported SHP2 small-mole activators only increase the phosphatase activity of SHP2 by twenty to thirty percent, while gain-of-function mutations of SHP2, which trigger leukemia, increase the activity of SHP2 by a thousandfold[40]. Thus, activating SHP2 to a low degree is expected to improve inflammatory diseases by exerting an anti-inflammatory effect with low cancer risk. In summary, as a negative regulator of inflammation, SHP2 has the potential to become a drug target for the treatment of inflammatory diseases. However, more SHP2 activators have to be identified to develop new strategies for anti-inflammatory therapy.

Due to the limited water solubility of oleanolic acid (<200 mmol/L), we encountered challenges in obtaining the co-crystal structure of the SHP2-E76K−OA complex, impeding a thorough exploration of the underlying mechanisms. Additionally, the low water solubility may hinder its biological availability. Consequently, our upcoming efforts aim to derive various compounds by chemically modifying oleanolic acid as the parent nucleus. This modification strategy is anticipated to enhance the compounds' solubility, favor co-crystallization, and potentially elevate their pharmacological activity.

5. Conclusions

In summary, the distinctive molecule oleanolic acid was shown to allosterically activate SHP2, resulting in selective inhibition of STAT3 signaling in T cells, effectively alleviating colitis in mice. These findings underscore the potential of oleanolic acid as a promising therapeutic agent for addressing Th17-related diseases.

Acknowledgments

This work was supported by the National Natural Science Foundation of China (82173820, 82073856, 82273933), Fundamental Research Funds for the Central Universities (020814380160, China), Innovation Team and Talents Cultivation Program of National Administration of Traditional Chinese Medicine (ZYYCXTD-C-202208, China), and the Young Scholar Foundation from Cyrus Tang Foundation (China).

Author contributions

Wenjie Guo, Wen Liu: Conceptualization, Funding acquisition. Jinbo Hu, Wen Liu: Investigation, Writing-Original draft preparation. Yi Zou: Visualization. Qiang Xu: Supervision. Chenyang Jiao, Jiazhen Zhu: Software, Validation. Yang Sun, Wenjie Guo, Jianjun Zou: Writing-Reviewing and Editing.

Conflicts of interest

The authors declare no conflicts of interest.

Appendix A. Supporting information

Supporting data to this article can be found online at https://doi.org/10.1016/j.apsb.2024.03.017.

References

1. Torres J, Mehandru S, Colombel JF, Peyrin-Biroulet L. Crohn's disease. *Lancet* 2017;**389**:1741−55.
2. Roda G, Chien Ng S, Kotze PG, Argollo M, Panaccione R, Spinelli A, et al. Crohn's disease. *Nat Rev Dis Prim* 2020;**6**:22.
3. Dipasquale V, Romano C. Genes *vs* environment in inflammatory bowel disease: an update. *Expet Rev Clin Immunol* 2022;**18**:1005−13.
4. Kumar A, Cole A, Segal J, Smith P, Limdi JK. A review of the therapeutic management of Crohn's disease. *Therap Adv Gastroenterol* 2022;**15**:17562848221078456.
5. Jefremow A, Neurath MF. Novel small molecules in IBD: current state and future perspectives. *Cells* 2023;**12**:1730.
6. Bakes D, Kiran RP. Overview of common complications in inflammatory bowel disease surgery. *Gastrointest Endosc Clin N Am* 2022;**32**:761−76.
7. Coulombe G, Leblanc C, Cagnol S, Maloum F, Lemieux E, Perreault N, et al. Epithelial tyrosine phosphatase SHP-2 protects against intestinal inflammation in mice. *Mol Cell Biol* 2013;**33**:2275−84.
8. Liu W, Guo W, Shen L, Chen Z, Luo Q, Luo X, et al. T lymphocyte SHP2-deficiency triggers anti-tumor immunity to inhibit colitis-associated cancer in mice. *Oncotarget* 2017;**8**:7586−97.
9. Zhao M, Guo W, Wu Y, Yang C, Zhong L, Deng G, et al. SHP2 inhibition triggers anti-tumor immunity and synergizes with PD-1 blockade. *Acta Pharm Sin B* 2019;**9**:304−15.
10. Guo W, Liu W, Chen Z, Gu Y, Peng S, Shen L, et al. Tyrosine phosphatase SHP2 negatively regulates NLRP3 inflammasome activation *via* ANT1-dependent mitochondrial homeostasis. *Nat Commun* 2017;**8**:2168.
11. Castellano JM, Ramos-Romero S, Perona JS. Oleanolic acid: extraction, characterization and biological activity. *Nutrients* 2022;**14**:623.
12. Yang W, Chen X, Li Y, Guo S, Wang Z, Yu X. Advances in pharmacological activities of terpenoids. *Nat Prod Commun* 2020;**15**:1−15.
13. Ayeleso TB, Matumba MG, Mukwevho E. Oleanolic acid and its derivatives: biological activities and therapeutic potential in Chronic diseases. *Molecules* 2017;**22**:1915.
14. Wang Y, Wei B, Wang D, Wu J, Gao J, Zhong H, et al. DNA damage repair promotion in colonic epithelial cells by andrographolide downregulated cGAS−STING pathway activation and contributed to the relief of CPT-11-induced intestinal mucositis. *Acta Pharm Sin B* 2022;**12**:262−73.
15. Wang Y, Wei B, Gao J, Cai X, Xu L, Zhong H, et al. Combination of fruquintinib and anti-PD-1 for the treatment of colorectal cancer. *J Immunol* 2020;**205**:2905−15.
16. Wei B, Xu L, Guo W, Wang Y, Wu J, Li X, et al. SHP2-mediated inhibition of DNA repair contributes to cGAS-sting activation and chemotherapeutic sensitivity in colon cancer. *Cancer Res* 2021;**81**:3215−28.
17. Liu W, Yang J, Fang S, Jiao C, Gao J, Zhang A, et al. Spirodalesol analog 8A inhibits NLRP3 inflammasome activation and attenuates inflammatory disease by directly targeting adaptor protein ASC. *J Biol Chem* 2022;**298**:102696.
18. Li Y, Liu N, Qian Y, Jiao C, Yang J, Meng X, et al. Targeting 14-3-3ζ by a small-molecule compound AI-34 maintains epithelial barrier integrity and alleviates colitis in mice *via* stabilizing β-catenin. *J Pharmacol Sci* 2023;**152**:210−9.
19. Tripathi SK, Lahesmaa R. Transcriptional and epigenetic regulation of T-helper lineage specification. *Immunol Rev* 2014;**261**:62−83.
20. Park H, Li Z, Yang XO, Chang SH, Nurieva R, Wang YH, et al. A distinct lineage of CD4 T cells regulates tissue inflammation by producing interleukin 17. *Nat Immunol* 2005;**6**:1133−41.
21. Fantini MC, Becker C, Monteleone G, Pallone F, Galle PR, Neurath MF. Cutting edge: TGF-β induces a regulatory phenotype in $CD4^+CD25^-$ T Cells through Foxp3 induction and down-regulation of Smad7. *J Immunol* 2004;**172**:5149−53.

22. Wu X, Guo W, Wu L, Gu Y, Gu L, Xu S, et al. Selective sequestration of STAT1 in the cytoplasm *via* phosphorylated SHP-2 ameliorates murine experimental colitis. *J Immunol* 2012; **189**:3497−507.
23. Jiang P, Zheng C, Xiang Y, Malik S, Su D, Xu G, et al. The involvement of TH17 cells in the pathogenesis of IBD. *Cytokine Growth Factor Rev* 2023;**69**:28−42.
24. Vahedi G, Takahashi H, Nakayamada S, Sun HW, Sartorelli V, Kanno Y, et al. STATs shape the active enhancer landscape of T cell populations. *Cell* 2012;**151**:981−93.
25. Yang XO, Panopoulos AD, Nurieva R, Chang SH, Wang D, Watowich SS, et al. STAT3 regulates cytokine-mediated generation of inflammatory helper T cells. *J Biol Chem* 2007;**282**:9358−63.
26. Murphy KM, Reiner SL. The lineage decisions of helper T cells. *Nat Rev Immunol* 2002;**2**:933−44.
27. Araki T, Nawa H, Neel BG. Tyrosyl phosphorylation of Shp2 is required for normal ERK activation in response to some, but not all, growth factors. *J Biol Chem* 2003;**278**:41677−84.
28. Loh ML. Mutations in *PTPN11* implicate the SHP-2 phosphatase in leukemogenesis. *Blood* 2004;**103**:2325−31.
29. Liu Y, Yang X, Wang Y, Yang Y, Sun D, Li H, et al. Targeting SHP2 as a therapeutic strategy for inflammatory diseases. *Eur J Med Chem* 2021;**214**:113264.
30. Guo W, Xu Q. Phosphatase-independent functions of SHP2 and its regulation by small molecule compounds. *J Pharmacol Sci* 2020;**144**:139−46.
31. Wang X, Zhang A, Gao J, Chen W, Wang S, Wu X, et al. Trichomide A, a natural cyclodepsipeptide, exerts immunosuppressive activity against activated T lymphocytes by upregulating SHP2 activation to overcome contact dermatitis. *J Invest Dermatol* 2014;**134**:2737−46.
32. Liu W, Wang M, Shen L, Zhu Y, Ma H, Liu B, et al. SHP2-mediated mitophagy boosted by lovastatin in neuronal cells alleviates parkinsonism in mice. *Signal Transduct Targeted Ther* 2021;**6**:34.
33. Hof P, Pluskey S, Dhe-Paganon S, Eck MJ, Shoelson SE. Crystal structure of the tyrosine phosphatase SHP-2. *Cell* 1998;**92**:441−50.
34. Chong PSY, Zhou J, Lim JSL, Hee YT, Chooi JY, Chung TH, et al. IL6 promotes a STAT3−PRL3 feedforward loop *via* SHP2 repression in multiple myeloma. *Cancer Res* 2019;**79**:4679−88.
35. Marasco MBA, Weyershaeuser J, Thorausch N, Sikorska J, Krausze, J, et al. Molecular mechanism of SHP2 activation by PD-1 stimulation. *Sci Adv* 2020;**6**:eaay4458.
36. Cao J, Huang YQ, Jiao S, Lan XB, Ge MH. Clinicopathological and prognostic significance of SHP2 and Hook1 expression in patients with thyroid carcinoma. *Hum Pathol* 2018;**81**:105−12.
37. Zhu Y, Wu Z, Yan W, Shao F, Ke B, Jiang X, et al. Allosteric inhibition of SHP2 uncovers aberrant TLR7 trafficking in aggravating psoriasis. *EMBO Mol Med* 2021;**14**:e14455.
38. Liu Q, Zhai L, Han M, Shi D, Sun Z, Peng S, et al. SH2 domain-containing phosphatase 2 inhibition attenuates osteoarthritis by maintaining homeostasis of cartilage metabolism *via* the docking protein 1/uridine phosphorylase 1/uridine cascade. *Arthritis Rheumatol* 2022;**74**:462−74.
39. Chan G, Kalaitzidis D, Usenko T, Kutok JL, Yang W, Mohi MG, et al. Leukemogenic *Ptpn11* causes fatal myeloproliferative disorder *via* cell-autonomous effects on multiple stages of hematopoiesis. *Blood* 2009;**113**:4414−24.
40. LaRochelle JR, Fodor M, Vemulapalli V, Mohseni M, Wang P, Stams T, et al. Structural reorganization of SHP2 by oncogenic mutations and implications for oncoprotein resistance to allosteric inhibition. *Nat Commun* 2018;**9**:4508.